Construction and Building Materials 379 (2023) 131166

Contents lists available at ScienceDirect

Construction and Building Materials

journal homepage: www.elsevier.com/locate/conbuildmat

Sorption isotherm measurements for porous materials: A new hygroscopic method

A. Taher *, H.J.H. Brouwers

Department of the Built Environment, Eindhoven University of Technology, P. O. Box 513, 5600 MB Eindhoven, the Netherlands

ARTICLE INFO

Keywords:
Salt solution method
Adsorption
Desorption
Manometric measuring method
Vacuum saturation method
Hygroscopic method

ABSTRACT

The water sorption of materials can significantly affect their durability. While a wide range of techniques has been already introduced and implemented to measure the sorption behavior of materials, obtaining high-resolution data to describe the water sorption isotherm is still a challenging task. This is especially the case for materials with a complex sorption behavior such as concrete for which the pore structure is very complicated. The level of complexity increases when chloride is present in such structures. In this study, a hygroscopic technique is introduced to measure the sorption behavior of porous materials. By this technique, the sorption isotherm can be obtained by injecting water with a high level of control into a controlled environment where a sample is positioned. The amount of water can be added in steps resulting in high-resolution data for the sorption properties of the sample. The technique is evaluated for two porous materials: Portland cement mortar and sand-lime brick. The results are extensively compared with similar measured data available in the literature. In addition, the performance of the technique is evaluated for porous materials with initial chloride content. The results show that the present technique allows for obtaining high-resolution data in desirable ranges that is essential for materials with complicated pore structures.

1. Introduction

The concrete durability is largely influenced by the level of corrosion of the steel rebars in the concrete structure. Corrosion in concrete structures usually occurs due to carbonatation and chloride penetration. Chloride penetration can be very important for structures on coastal areas where chloride concentrations in the water and the air is rather high. This is also the case for concrete roads and bridges when de-icing salt is used to prevent roads from icing. It is, therefore, essential to better understand water and chloride transport in concrete structures. Water and chloride transport in concrete is very complicated as it depends on several parameters such as the sorption isotherm [1–2], porosity [3], permeability, diffusion coefficient of water [4] etc.

Sorption isotherm is defined as the relationship between water content and humidity of a material at thermodynamic equilibrium. Different approaches have been implemented to investigate the sorption of water in different materials. For example, saturated salt solution method [5–10], hygroscopic method [11], manometric measuring method [12], nuclear magnetic resonance (NMR) [13–14], etc. The advantages and disadvantages of these methods are summarized in Table 1, based on the information provided in Refs. [5–19].

The saturated salt solution, hygroscopic and manometric measuring methods are widely used for research on sorption isotherm properties of porous materials such as concrete.

The simplest method is by direct weighing of the sample. A sample of known size and mass is kept in an environment of known humidity and weighed times as the humidity is increased. The adsorption and desorption of water by several materials, including concrete, have been widely investigated using this technique [5–9]. Although this approach can be easily implemented, errors can often occur due to the interruption of the sorption process at each weighing. Several studies have been performed to minimize errors associated with the weighing method. For example, Crank and Park [18] used a quartz spring method in which the increase of mass of the sample due to the adsorption of vapor is obtained from the length of the spring. Other studies proposed to measure the increase in mass of the sample using a balance [19].

The hygroscopic approach is an alternative approach, which is used to measure the sorption isotherm of water in very thin layers of paint. In this approach, the sample is initially dried completely and then is placed inside a glass jar. The jar has two openings to let the air go through the

* Corresponding author.
E-mail addresses: a.taher@tue.nl, azee1@live.nl (A. Taher).

https://doi.org/10.1016/j.conbuildmat.2023.131166
Received 17 September 2022; Received in revised form 22 February 2023; Accepted 21 March 2023

Table 1
Advantages and disadvantages of different sorption isotherm methods [5–19].

Method	Advantages	Disadvantages
Saturated salt solution	- Minimizing temperature fluctuation - Easy to use	- Low-resolution data - Time-consuming
Manometric	- High precision	- Time-consuming - Limited pressure range - Limited sample size
Hygroscopic	- Accurate - High-resolution data	- Time-consuming
Nuclear magnetic resonance	- Accurate - High-resolution data	- Expensive equipment - Limited sample size

jar. Water drops are injected into the jar to create various relative humidity conditions. The air temperature and relative humidity inside the jar are measured when an equilibrium between the environment and the sample is achieved. In this case, one point on the sorption isotherm curve is obtained. This procedure can be continued until the saturation is almost reached. In this approach, the desorption curve is obtained as follows: A saturated sample is placed inside the jar. Air with a relatively low relative humidity is induced into the jar with a certain flowrate and time interval duration. The sample will release water due to the decrease in relative humidity caused by the dry air. Equilibrium is reached after a while and a point on the curve is obtained the same way as described before.

The manometric technique is a volumetric measurement technique [12], in which two chambers of the known volume are used. A valve separates the chambers from each other. The pressure in the chambers is measured using a manometer, the temperature can be controlled by any temperature-controlling system. At the start of the experiment, the sample is placed in the chamber, while a valve is opened to fill the other chamber with air containing vapor to an initial pressure. Then the valve between the chambers is opened, allowing the second chamber containing the sample to fill with air containing vapor. Any drop in pressure beyond that due to the volume difference between the first chamber and the two chambers together is assumed to be the consequence of the sample adsorbing water. The amount of water adsorbed by the sample is then obtained using the real gas law.

Penetration of chloride solution into porous materials is of interest in a wide range of applications. The presence of chloride in the pores of a material can change the physical properties of the material [20]. This phenomenon can also affect the contact angle and surface tension of the water. Therefore, one can expect that the presence of chloride will significantly affect water transport in porous materials such as concrete [21,22]. Since sorption takes place on the surface of the pores, the presence of compounds strongly influences the sorption isotherm.

Rijniers [23] has measured the sorption isotherm of bulk salts, one of which was NaCl. It is found that the sodium chloride adsorbs no water vapor up until a high relative humidity (±75%). At this high relative humidity, the salt turns into a salt solution and adsorb a large amount of water vapor. Franzen and Mirwald [24] have investigated the effect of chloride on the water uptake in sand-lime samples. From humidity sorption experiments, it is concluded that samples treated with different chloride mixtures have an extremely increased water uptake. At a relative humidity of about 70%, the samples tend to absorb a large amount of water. Koniorczyk and Wojciechowski [25] measured the sorption isotherm of cement mortar with different sodium chloride contents and created a model based on neural networks. The results showed that the higher the chloride content, the more water is absorbed. It was also observed that the presence of chloride can affect the drying time of the material. In this case, the drying time of the material containing chloride, compared with the case with water, was longer. This can be explained with the effect of chloride on the hygral state of the material. It should be noted that chloride can also change the effective conductivity, but also the thermal capacity of the multiphase domain, which influences the energy transport. Additionally, energy is released or consumed during phase change. Villani et al. [26] predicted and measured the diffusivity of deionized water and various chloride solutions in mortar. It is seen that the diffusivity of a 17% NaCl-solution is larger than the diffusivity of deionized water, particularly at high relative humidities.

In this study, the hygroscopic method described by Van der Zanden and Goossens [11] is chosen, because it allows measuring more points of the sorption isotherm than other techniques. The accuracy of the measurements is also adjustable by adding extra water in the experiment. Adjusting the accuracy of the results is important for materials with a complicated pore structure such as concrete. Here, the sorption isotherm of two porous materials, mortar and sand-lime, are measured and compared with literature. The effect of chloride in mortar samples is also studied by comparing the sorption isotherms of a sample containing chloride and a sample free of chloride.

2. Materials and sample preparation

2.1. Sample preparation

In this experiment, two porous materials are studied. (i) cement-based mortar specimens and (ii) sand-lime specimens. The cement in this study have a chloride content of $\leq$ 0.1% by the mass of the final cement according to EN 197–1 and that is neglected, because of the very small quantity. PVC cylinder tubes with a diameter 100 mm are used to cast mortar. After curing the mortar for 28 days, the cylinder samples are cut in pieces with a thickness of 10 mm. The porosity of the samples is measured using the vacuum-saturation technique following the standards NT Build 492 [27] and ASTM C1202 [28]. More detailed information about the the test procedure is provided in Yu and Brouwers [29]. Therefore, only highlights are briefly presented here:

1) The samples are placed in a dessicator and apply a pressure of 4 kPa for 3 h;
2) The dessicator is filled with water gradually until the sample is completely immersed in water;
3) The pressure is maintained for an additional hour;
4) The samples are left in water for 18 h;
5) The mass of the surface dry samples in air is measured;
6) The mass of the samples in water is measured;
7) The sample is dried in an oven at 50 °C until a constant mass is reached. The mass of the sample is then measured.

The porosity of the samples is calculated using equation:

$$\varphi_{v,water} = \frac{m_s - m_d}{m_s - m_w} \times 100 \quad (1)$$

where $\varphi_{v,water}$ is the porosity (%), m_s is the surface dried mass of water saturated sample in air (g), m_w is the mass of water-saturated sample in water (g), and m_d is the mass of oven dried sample (g). Based on these measurements, the mortar and sand lime samples have a porosity of 17% and 32%, respectively, as shown in Fig. 1.

Based on the measured porosity, a salt solution of four liters is prepared by dissolving 237 g sodium chloride per liter distilled water, to provide the samples with chloride concentration of 2%. For the sand-lime measurements, cylindrical samples were extracted from the sand-lime block. In this case, the diameter and the thickness of the samples are 100 mm and 10 mm, respectively. Fig. 2 shows the measured compressive and flexural strength of the mortar sample. The specifications of the two porous materials are presented in Table 2.

After completing the preparation of the salt solution, all the samples

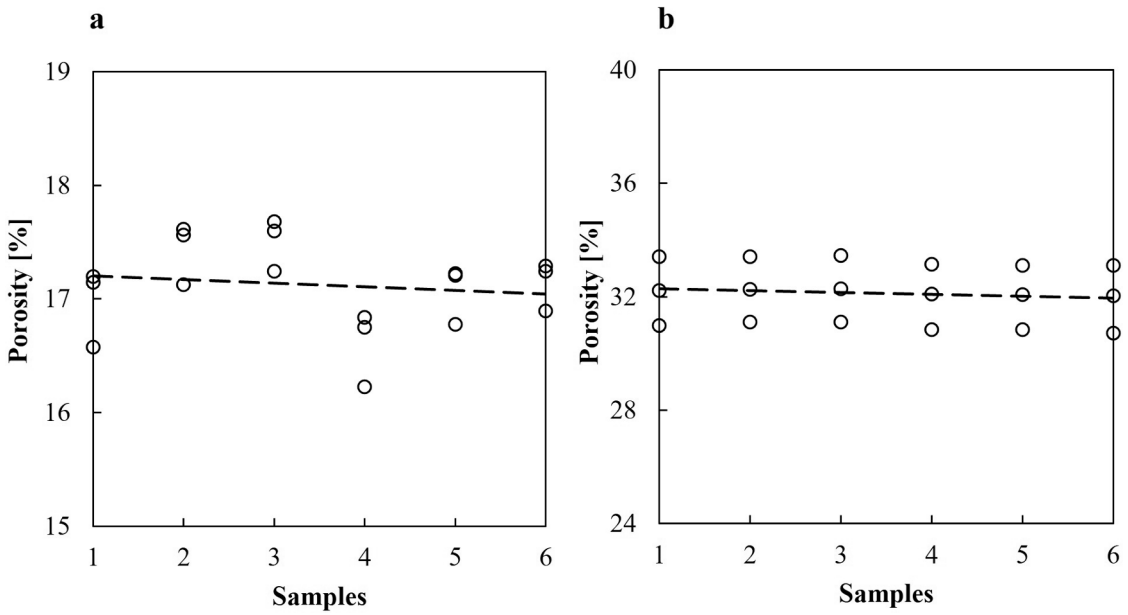

Fig. 1. The measured porosity of (a) mortar samples, and (b) sand-lime samples following the standards NT Build 492 (1999) and ASTM C1202 (2005).

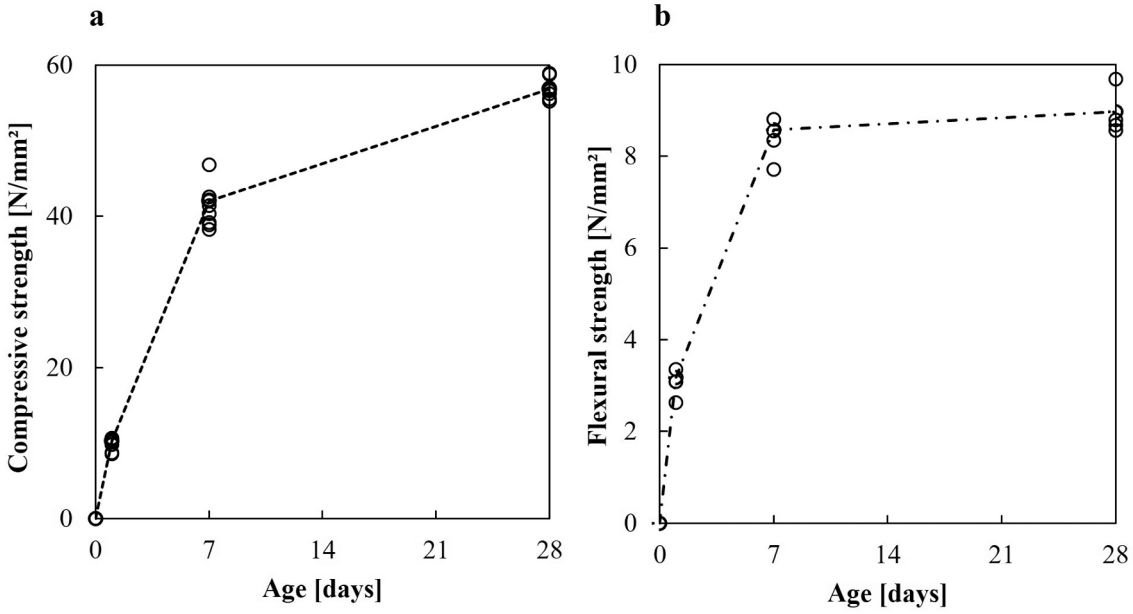

Fig. 2. (a) Compressive strength, and (b) flexural strength of mortar samples.

Table 2
Main characteristics of mortar and sand-lime.

Materials	Mortar Volume [m^3]	Mass [kg]	Sand-lime
CEM I 42,5N	159.5	502.2	–
Sand	568.5	1506.5	–
Water	251.1	251.1	–
Superplasticizer	0.9	1	–
Air	20	–	–
w/c	0.5		–
Porosity / 28-day	17%		32%
Class	–		CS12
Production	–		25-May-2011
Compressive strength / 28-day	56.8 MPa		12 MPa
Flexural strength / 28-day	8.9 MPa		–

are placed in a holder in a desiccator (Fig. 3). The vacuum saturation method is implemented in order to saturate the samples with the chloride solution. To do so, the following steps are taken:

1) A vacuum suction (4 kPa) is applied using a pump for 3 h for de-airing the samples.

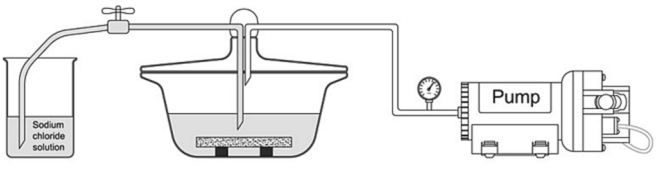

Fig. 3. Penetrating chloride into the specimens using vacuum saturation.

2) The chloride solution is added in order to have an initial concentration level of chloride in the samples.
3) The vacuum suction is maintained for another hour to ensure that the air void inside the sample is entirely satuared with the chloride solution.
4) Finally, before the chloride concentration profiles are measured, the samples will be maintained in the chloride solution at the laboratory conditions for a three- day period.

Profiles of the chloride concentration are determined by titration to examine the chloride penetration into the sample.

2.2. Titration analysis

In this study, the titration analysis is used to measure the chloride concentration profiles. The titration analysis is a very popular method for chemical analysis [30–33].

Potentiometric titration curves are obtained by plotting the potential of the indicator electrode E against the volume V of the added titrant. Rapid changes in the potential signal the equivalence point of the titration. The maximum change in potential is calculated by finding the maximum slope of this graph. This is easily found by plotting the first derivative curve dE/dV against V, the equivalence point is the point where dE/dV is zero. The corresponding value for the added titrant is thus obtained, the volume of the analyzed solution is known, which is set to 10 mL, and so the concentration of the analyte is calculated. With automatic titration, these calculations are done by a computer.

2.3. Chloride concentration profiles

To obtain chloride concentration profiles, layers of three mortar samples (numbered 1, 2 and 3) are ground with Profile Grinder 110 as shown in Fig. 4. On the outer 2 mm of the sample, layers of 1 mm are ground, the rest of the sample is ground into layers of 2 mm. The powder is collected in marked plastic bags.

Due to the pressure caused by the placeholder on sample 1, the last 2 mm were cracked before grinding. Therefore, the last 2 mm is regarded as one layer.

The powder of the three samples is placed in cups per layer and dried in an oven at 100 °C for 24 h.

After the powder is dried for at least 1 day, chemical analysis is performed as follows:

1) 2 g of each layer is weighed and placed in a beaker.
2) 35 mL of distilled water and 2 mL nitric acid of 1 M is added to the beaker.
3) The content in the beaker is mixed for 1 min.
4) The mixture is placed on a hot plate, brought to boiling and cooled afterward.
5) The content is poured onto filter paper in order to separate fine substances from the mixture. For each set of measurements, 100 mL of the filtered mixture is captured, of which only 10 mL is used to determine the chloride concentration profiles.
6) The measurement is performed by an automatic titration device, Metrohm MET 702 in which the principle of potentiometric precipitation titration is applied (Fig. 5). This principle determines the chloride concentration by potentiometric titration with silver nitrate (titrant) and a silver electrode (indicator electrode).

For each layer, two sets of measurements are done. The resulting chloride profiles are shown in Table 3 and Fig. 6, in which the chloride concentration is presented as a function of distance from the surface of the samples.

It should be noted that the sample is not sealed at the top and the bottom surfaces. Therefore, the chloride can penetrate through both surfaces easily, while it was more difficult to move to the deeper level of the sample. In addition, the samples in the experiments were not completely dried before placing them in the sodium chloride solution. Therefore, it is expected that the chloride concentration would be higher throughout the samples and less sensitive to the depth of samples if the samples were firstly dried completely.

2.4. Chloride concentration profiles in completely dried samples

An additional experiment is performed, in which three samples are first completely dried using an oven at 50 °C and relative humidity of 10%. The same procedure, as described in Section 2.3, is used to determine the chloride concentration profiles of the dried samples. From the obtained results in Fig. 7 and Table 4 it is indeed seen that drying the samples completely before placing in the salt solution gives higher values and more uniform chloride concentration profiles within the depth of the samples.

One can expect to see a symmetric distribution of the concentration in the samples, since the samples are assumed to be homogeneous. However, this is not the case, and differences in the chloride concentrations are clearly observed (see Fig. 7). The main reason for these differences is not clear. But it could be probably caused in the stage of grinding layers of the samples. The samples are fixed by a holder, which disables the sample to move during the grinding process. This fixing causes stress in the sample, which causes the formation of cracks when

Fig. 4. Profile Grinder 110 device.

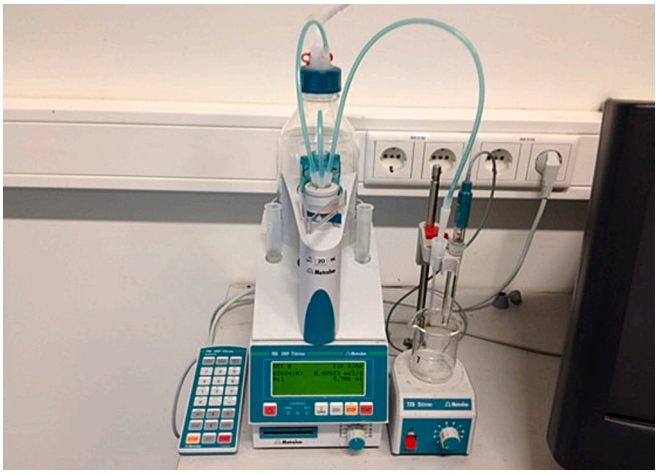

Fig. 5. Metrohm MET 702 automatic titration device.

Table 3
The chloride concentration of ground layers from three samples, obtained from two measurements.

	Chloride concentration [%]			
	Profile [mm]	Measurement 1	Measurement 2	Mean concentration
Sample 1	0–1	1.246	1.241	1.2435
	1–2	0.880	0.883	0.8815
	2–4	0.633	0.625	0.6290
	4–6	0.479	0.478	0.4785
	6–8	0.606	0.611	0.6085
	8–10	0.850	0.859	0.8545
Sample 2	0–1	1.280	1.289	1.2845
	1–2	0.942	0.928	0.9350
	2–4	0.649	0.643	0.6460
	4–6	0.432	0.427	0.4295
	6–8	0.527	0.520	0.5235
	8–9	0.771	0.769	0.7700
	9–10	0.973	0.975	0.9740
Sample 3	0–1	1.250	1.255	1.2525
	1–2	0.897	0.898	0.8975
	2–4	0.588	0.587	0.5875
	4–6	0.370	0.369	0.3695
	6–8	0.412	0.408	0.4100
	8–9	0.583	0.593	0.5880
	9–10	0.768	0.771	0.7695
	10–11	1.077	1.095	1.0860

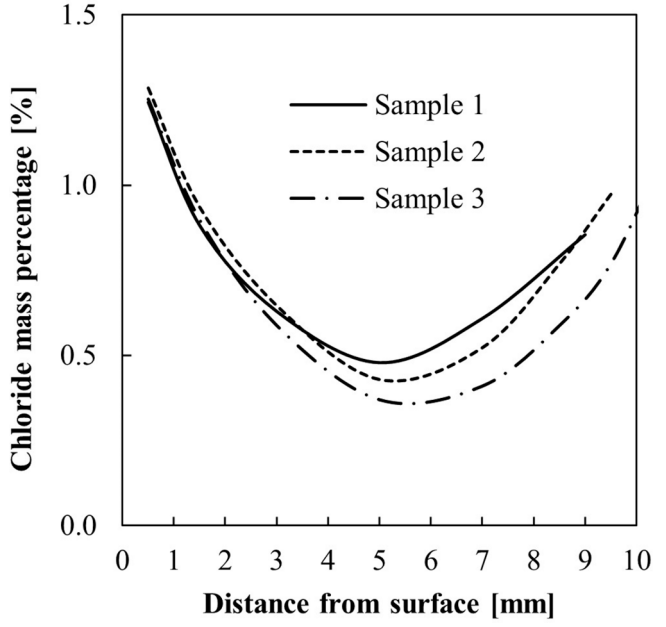

Fig. 6. Measured concentration profiles as a function of depth for mortar samples. For all smaples, the thickness is 10 mm.

its thickness is small, i.e. in the last layers. Cracking of the sample leads to less pulverized layers, with larger particles. Due to this rather coarse powder, the chloride bound to the surface of the pores is less dissolved when water and nitric acid are added to the powder. This yields an erroneous chloride concentration. It is thus assumed that the chloride concentration on the right side of the graph, where the obtained powder was rather coarse, is equal to the left side of the sample.

2.5. Determining the effectiveness of the vacuum saturation method

To verify the effectiveness of the vacuum saturation method, three

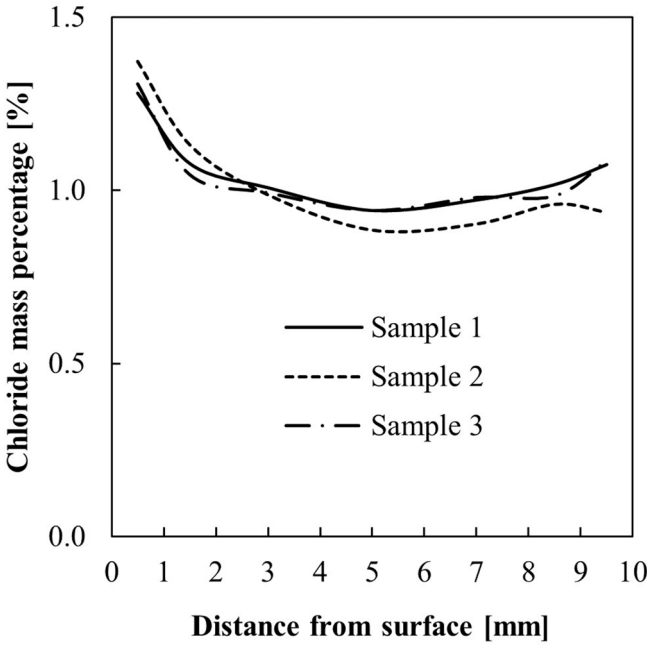

Fig. 7. Experimentally obtained chloride concentration profiles, where samples were completely dried before measurement.

Table 4
The chloride concentration of ground layers, where samples were completely dried before measurement.

		Chloride concentration [%]		
	Profile [mm]	Measurement 1	Measurement 2	Mean concentration
Sample 1	0–1	1.285	1.277	1.2810
	1–2	1.074	1.080	1.0770
	2–4	1.010	1.004	1.0070
	4–6	0.940	0.942	0.9410
	6–8	0.978	0.965	0.9715
	8–9	1.019	1.013	1.0160
	9–10	1.074	1.074	1.0740
Sample 2	0–1	1.371	1.372	1.3715
	1–2	1.129	1.132	1.1305
	2–4	0.993	0.979	0.9860
	4–6	0.876	0.892	0.8840
	6–8	0.893	0.910	0.9015
	8–9	0.958	0.959	0.9585
	9–10	0.936	0.935	0.9355
Sample 3	0–1	1.308	1.307	1.3075
	1–2	1.044	1.046	1.0450
	2–4	0.990	0.995	0.9925
	4–6	0.944	0.939	0.9415
	6–8	0.979	0.979	0.9790
	8–9	0.985	0.982	0.9835
	9–10	1.080	1.090	1.0850

mortar samples are prepared, having a thickness of 10, 20 and 40 mm. These samples are dried first using a climate chamber, in which air of 50 °C and relative humidity of 10% is blown over the samples. The samples are weighed every day until a constant mass is reached. The samples are then placed in the glass jar. The same procedure, as described in Section 2, is then followed to saturate the samples. Note that in these experiments distilled water is used (instead of chloride solution), and the samples are maintained in the water for 24 h instead of 3 days. If the method of vacuum saturation would indeed remove all the air out of the samples, the specific increment in mass after 24 h

would be the same for each sample, regardless of its thickness. The results are shown in Table 5.

It can be seen that the mass increment of the three samples is almost equal, being in the order of 7% of its original mass. This result gives rise to the assumption that the vacuum saturation method removes all the air out of the samples and saturates the pores with liquid.

3. Methodology

The sorption isotherm consists of two curves: (i) one that indicates the history of wetting, i.e. adsorption of water and (ii) one that indicates the history of drying, i.e. desorption of water. It should be noted that in some cases, depending on the properties of the material such as the porosity and permeability, these two curves are not identical. This is especially the case for concrete.

3.1. Adsorption isotherm

For the adsorption curve, a sample is completely dried in the climate chamber and then is placed in a glass jar with two sensors for relative humidity temperature as shown in Fig. 8. The glass jar is kept inside a room with a temperature-controlled environment. The temperature of the room is about 21 °C. Each data point is collected when the humidity inside the jar does not change (i.e. equilibrium). In order to prevent leakage in the system, a Teflon ring is used as a closure.

The sample is placed first in the jar and since the sample still contains a small (unknown) amount of water, an initial equilibrium is awaited. This initial equilibrium state is the origin of the sorption curve. After the initial equilibrium is reached, a detailed sensitivity analysis is performed to assess the impact of the amount of water added to the jar on the accuracy of the experiments. To reach this goal, three quantities are tested: (i) 0.1 mL (ii) 0.3 mL and (iii) 0.5 mL of water are added to the jar. For the case with 0.1 mL of water, the experiment takes about 4 days to reach an equilibrium. However, this could provide detailed information about the absorption behavior of material if needed. Note that larger quantities could be used in parts of the curve where detailed information is less significant, while this could shorten the experimental duration.

The combination of using different quantities of water can be used until a final equilibrium is reached. Fig. 9 shows how relative humidity changes as a function of time. It can be seen that the profile of relative humidity can be divided into three phases. The first phase is the increase of the relative humidity which is the result of the evaporation of the injected water. In the second phase, the relative humidity reduces due to the adsorption of the porous material. The final phase is the equilibrium state between the relative humidity inside the jar and the adsorbed water of the sample.

The adsorption isotherm is calculated by measuring the amount of water in the system and in the air. The relationship between these two quantities and the amount of water inside the sample is given by:

$$m_{sample} = m_{total} - m_{air} \tag{2}$$

where m_{total} is the amount of water in the system, and m_{air} is the amount of water in the air that is measured based on the relative humidity. The amount of water inside the sample, m_{sample} , then can be obtained using Eq. (1).

By implementing the Antoine equation and the ideal gas law, the concentration of water in the saturated air, C_{sat} (kg/m^3) can be calculated as follows:

$$C_{sat} = \frac{M}{R \cdot T} \cdot e^{\left(A - \frac{B}{C+T}\right)} \tag{3}$$

where M (kg/mol) is the molar mass of water, R (J/(K·mol)) the gas constant and T (K) the temperature, and A (=23.19695), B (=3816.44) and C (=-46.13) are constants [34–35]. The concentration of water inside the jar can be computed based on the measured relative humidity (RH) inside the jar as follows:

$$C = \frac{RH}{100} \cdot C_{sat} \tag{4}$$

From Eqs. (2) and (3), the mass of water in the air inside the jar can be obtained using:

$$m_{air} = C \cdot V \tag{5}$$

where V is the volume of the jar.

At a specific relative humidity, the water content (kg/m^3) in the

Table 5
The determination of the accuracy of vacuum suction.

	Sample 1 (10 mm)	Sample 2 (20 mm)	Sample 3 (40 mm)
Dry mass [g]	179.68	349.45	691.80
Mass after desiccation and wetting [g]	192.45	374.00	739.90
Mass increment [%]	7.11	7.03	6.95

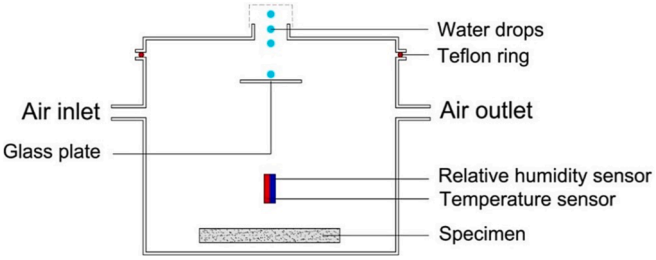

Fig. 8. Experiment set-up to measure the sorption isotherm of porous material with a hygroscopic method.

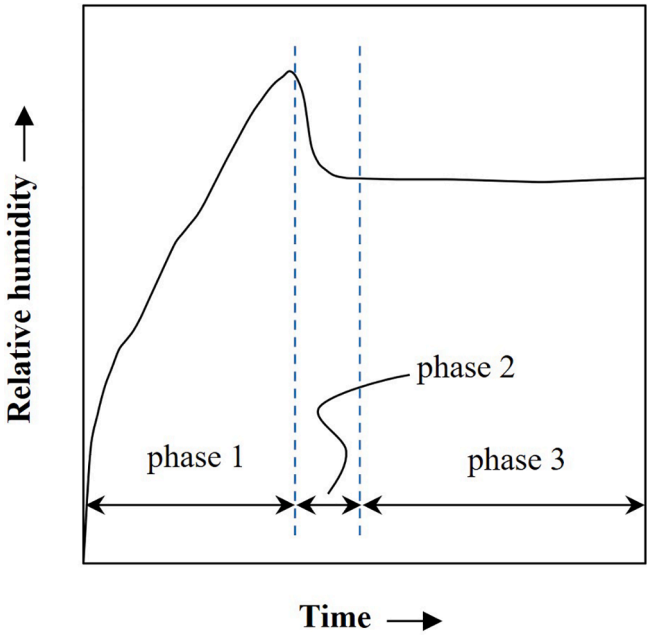

Fig. 9. Characteristic chart of the humidity in the vessel as a function of time. The chart can be divided into three phases; the first phase is the increase of the relative humidity which is the result of the evaporation of the injected water. The second phase is the decrease of the relative humidity that results from the adsorption of the porous material. The final phase is the equilibrium state between the relative humidity inside the vessel and the adsorbed water of the specimen.

sample can be obtained by dividing the mass of water in the sample (m_{sample}, obtained using Eq. (1)) by the volume of the sample.

3.2. Desorption isotherm

When the final equilibrium, at a relative humidity of approximately 90%, is reached the determination of the desorption isotherm is started. At this stage, the mass of water in the sample, as well as the mass of water in the air of the jar, are known. Fig. 10 shows how relative humidity changes as a function of time. This graph can be divided into three phases. In the first phase, the relative humidity decreases, which is due to the blowing dry air into the jar. The second phase is the increase of relative humidity resulting from the release of water by the sample. The final phase (phase 3) is the equilibrium state between the water in the air of the jar and the water in the sample.

The desorption curve can be determined by pumping dry air into the jar for a certain amount of time. If the removed amount of water during the drying process is calculated, one point of the desorption curve can be determined. By using a mass balance, the mass of water removed from the jar is calculated as

$$m_{out} = \int_0^{\tau} \varphi_v (C_{out} - C_{in}) dt \quad (6)$$

where φ_v is the volumetric flow of the dry air and τ is the elapsed time of blowing air in the jar. In this equation, C_{out} and C_{in} are water concentration for the air leaving and entering the jar, respectively. By combining Eqs. (3) and (5), m_{out} can be rewritten as follows:

$$m_{out} = \frac{C_{sat}\varphi_v}{100} \int_0^{\tau} (RH_{out} - RH_{in}) dt \quad (7)$$

where RH_{out} and RH_{in} are the relative humidity of air leaving and entering the jar, respectively. Equilibrium is awaited, then the mass of water in the air at equilibrium is calculated with Eqs. (3) -(5). The water content in the sample is calculated from a mass balance between the mass of water in the system, and in the air inside the jar. It should be noted at each step, the mass of water in the system is obtained by subtracting the total amount of water in the jar (system) at the previous step from m_{out}, obtained by Eq. (6).

It is initially assumed that the jar is an ideal mixer, implying that the humidity at the outlet is the same as the humidity in the core of the jar. Therefore, the humidity of the leaving air is equal to the measured humidity inside the jar. It is, however, observed that this assumption is associated with errors. This is because, given the location of the sensor of relative humidity in the jar, the measured values cannot be representative of the relative humidity of air leaving the jar. This error is eliminated by adding a sensor of relative humidity in the tube through which the air leaves the jar. In this case, the relative humidity is measured of air leaving the jar (RH_{out}) can be measured more accurately.

4. Results

Fig. 11 shows the obtained sorption isotherm for the mortar sample for both cases: with and without chloride. For the case with chloride, the figure shows the adsorption and desorption behavior of the sample. It can be seen that for the entire range of the tested relative humidity, the adsorption of the sample containing chloride is larger than the sorption of the sample containing no chloride. This is more significant for the higher values of relative humidity. For example, for RH = 20%, the absolute difference is about 4 kg/m^3, while this difference goes up to 37 kg/m^3 for RH = 70%. In addition, a closer look at Fig. 11 reveals that the adsorption curve for the case without chloride is almost linear. On the other hand, for the sample containing chloride, a BET-Type-II curve is clearly observed [36–37]. The significant increase in the adsorption properties of the case containing chloride is due to the fact that some chloride can be bound to the surface of the pore walls. The bounded chloride is then capable of absorbing some water. This phenomenon, therefore, can significantly increase the adsorption properties of the material.

Earlier studies have shown that the presence of chloride, but also the pore size distribution can significantly influence the sorption isotherm. For example, Villani et al. [26], based on the study by Benavente [38–39] Selander [40] and Spragg [41], developed a thermodynamical model, in which an equilibrium relative humidity is derived as:

$$RH_{eq}(r) = a_w e^{\frac{2\sigma v_l^0}{rRT}\cos\phi} \quad (8)$$

where a_w is the water activity [-], σ is the surface tension [N/m], v_l^0 is the molar volume of the liquid [m^3/mol], R is the universal gas constant [N.

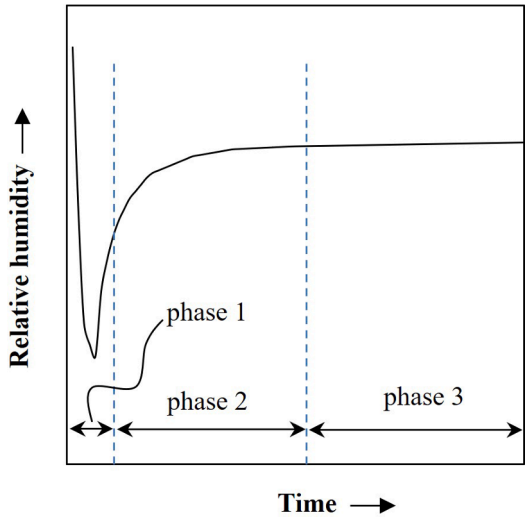

Fig. 10. Characteristic chart of the humidity in the vessel as a function of time. This chart can be divided into three phases; the first phase is the decrease of relative humidity which results from blowing dry air in the vessel. The second phase is the increase of relative humidity resulting from the release of water by the sample. The final phase is the equilibrium state between the water in the air of the vessel and the water in the sample.

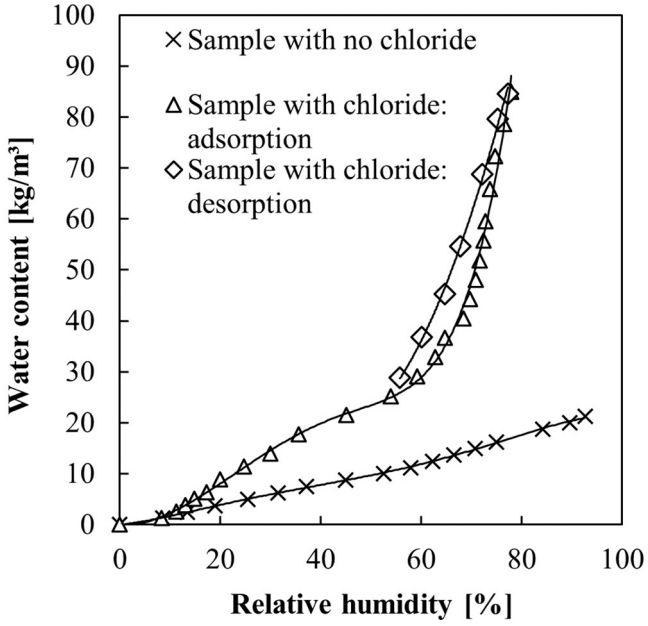

Fig. 11. Comparison of sorption between a mortar sample containing chloride and a sample containing no chloride.

m/K.mol], T is the temperature [K], r is the pore radius [m] and Φ is the contact angle [deg]. According to this model, the presence of chloride can change the properties of the material such as the equilibrium relative humidity. This is mainly because the chloride content will change the surface tension of the material. It should be noted that although the surface tension of a sodium chloride solution is higher than the surface tension of pure water, the water activity is lower. For a given pore radius, this will make the equilibrium relative humidity of samples lower than that of pure water. In this perspective, if the environmental relative humidity is lower than the equilibrium relative humidity, water evaporates. If the environmental relative humidity is higher, condensation occurs. Thus, if the equilibrium relative humidity in a pore is lower, condensation occurs at lower relative humidity. This can be an explanation for the increased sorption of a sample containing sodium chloride.

It should be noted that the linear behavior of adsorption isotherm for mortar containing no chloride can also be seen in the studies by Tada and Watanabe [42], Daina [43] and Pel [44]. Fig. 11 also shows the desorption behavior of the mortal sample for the case containing chloride, where the hysteresis effect can be clearly observed.

It is interesting to compare the water absorption prion measured here with those measured by [44] using NMR. Here the mortar samples has a water:cement:sand composition of w:c:s = 0.5:1:3, whereas in [44] the composition was w:c:s = 0.5:1:5.6. Thus means that our sample and that of [44] have a different paste and hydrated cement content, which needs to be accounted for.

The hydrated cement volume fraction, which is the phase that absorbs water, in the cement paste can expressed with the Powers and Brownyard model as [45,46]:

$$\varphi_{hp,p} = \frac{\alpha\left[\frac{\nu_c}{\nu_w} + \frac{w_d \nu_d}{\nu_w c}\right]}{\frac{\nu_c}{\nu_w} + \frac{w}{c}} \tag{9}$$

with α as degree of cement hydration, ν_c/ν_w and ν_d/ν_w the ratios of specific volume of cement and water (≈ 0.32) and of total bound water and free water (≈ 0.81), respectively, and the w_d/c the mass of this total bound water (chemically and physically bound) per mass of cement (≈ 0.4). The volume of the cement paste in the mortar reads:

$$\varphi_{p,m} = \frac{\frac{\nu_c}{\nu_w} + \frac{w}{c}}{\frac{\nu_c}{\nu_w} + \frac{w}{c} + \frac{\nu_s s}{\nu_w c}} \tag{10}$$

with ν_s/ν_w the ratio of specific volume of sand (mostly quartz) and water (≈ 0.38). The volume fraction of hydrated cement in mortar reads:

$$\varphi_{hp,m} = \varphi_{hp,p}\varphi_{p,m} = \frac{\alpha\left[\frac{\nu_c}{\nu_w} + \frac{w_d \nu_d}{\nu_w c}\right]}{\frac{\nu_c}{\nu_w} + \frac{w}{c} + \frac{\nu_s s}{\nu_w c}} \tag{11}$$

In [44] and here, the same type of cement was used (OPC, CEM I), so with same ν_c/ν_w and w_d/c, and if we assume a similar degree of hydration, the present results and those of [44] become comparable by assessing their denominator of Eq. (11) only, being 1.96 and 2.95, respectively. The later value expresses that the paste content is lower in the mortar of [44], as more sand was mixed in.

Fig. 12 compares the adsorption isotherm of the mortar sample without added chloride as obtained in the present study, with those of "Fig. 4.8" in [44], where the values have been multiplied by 2.95/1.96 = 1.5 to compensate for the lower cement paste content. It can be seen that for all relative humidity values, the results of the presented method and [44] are close to each other, though here slightly higher adsorption isotherm values are obtained.

Fig. 13 shows the adsorption of sand-lime samples for both with and without chloride. The properties of the material are presented in Table 2. Similar to the mortar sample, for the sand-lime samples higher adsorption properties are also obtained for the case containing chloride. However, the effect of the presence of chloride is less significant. For example, for RH = 20% and RH = 70%, the absolute difference is about

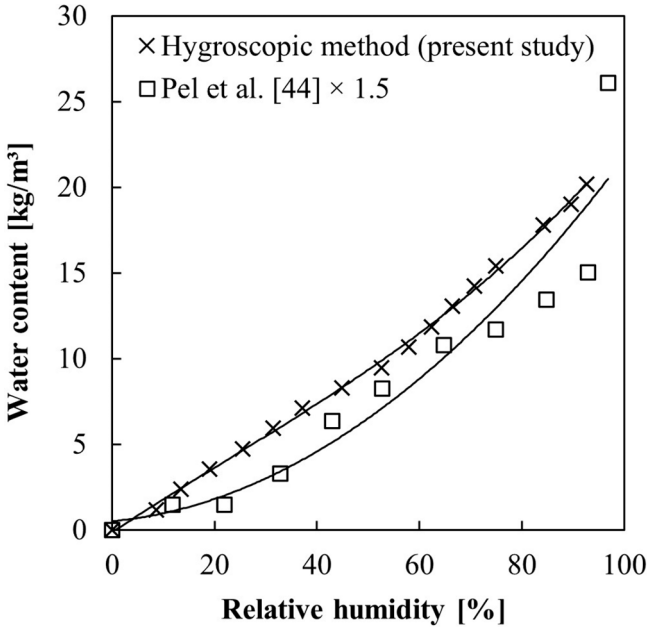

Fig. 12. Adsorption isotherm of mortar sample containing no chloride.

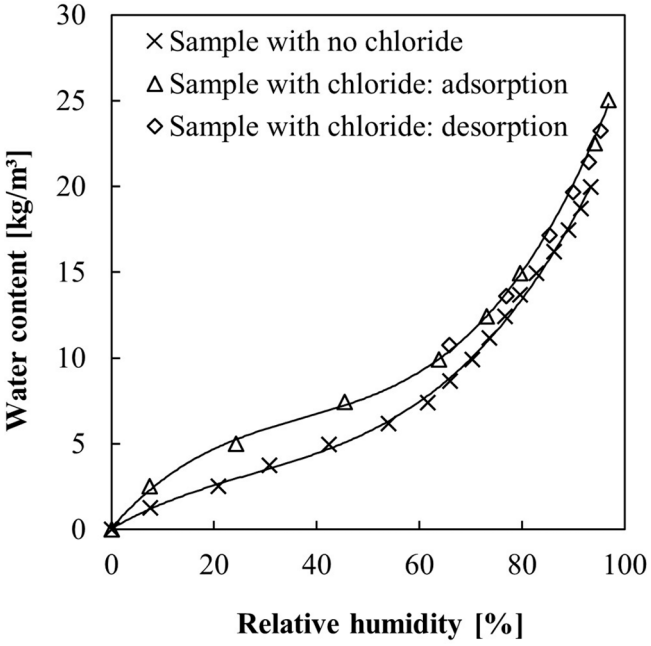

Fig. 13. Comparison of sorption between a sand-lime sample containing chloride and a sample containing no chloride.

2.1 kg/m^3 and 1.8 kg/m^3, respectively. In addition, for both cases, the adsorption curves are BET Type II.

The difference in the adsorption properties of sand-lime with and without chloride is in line with the results of the previous studies by Rijniers [23] and Franzen and Mirwald [24]. The main reason for such differences can be related to the tendency of chloride to adsorb water [9–10].

Furhtemore, Fig. 13 also shows the desorption curve for sand-lime containing chloride. No hysteresis effect can be observed for the sand-lime material.

The adsorption isotherm of the sand-lime sample with no chloride is also compared with the results provided by Pel [44], as shown in Fig. 14. Similar trends can be seen in the behavior of the adsorption properties as

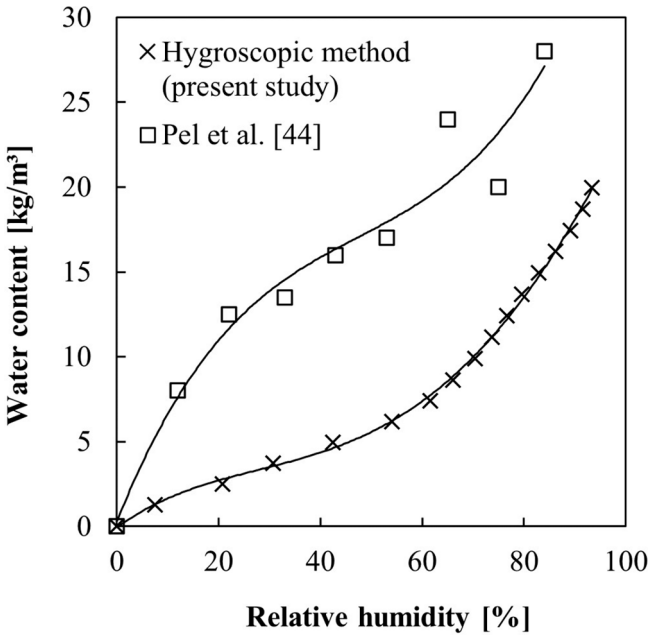

Fig. 14. Adsorption isotherm of sand-lime containing no chloride.

a function of relative humidity. In [44] no speficic details on the used sand-lime sample could be found, so that there may be a difference in used samples, so the sample used here and that in [44]. Obvious;ly, a difference in materials will lead to a different outcome in adsorption properties.

5. Conclusions

In this study, a hygroscopic technique is introduced to measure the sorption behavior of porous materials. To the best knowledge of the authors, the accuracy of the hygroscopic technique has not yet been investigated for porous materials. Therefore, this study introduces a novel hygroscopic technique to measure the sorption behavior of porous materials. In this technique, the sorption isotherm can be obtained by injecting water with a high level of control into a controlled environment where a sample is positioned. The amount of water can be added in steps resulting in high-resolution data for the sorption properties of the sample.

The technique is evaluated for two porous materials: Portland cement mortar and sand-lime brick. The results are extensively compared with similar measured data published in the literature. Given the fact that the presence of chloride can significantly increase the level of complexity of the sorption behavior of porous materials, in this study, the performance of the new technique is also investigated for samples containing chloride.

It is found that the samples containing chloride have higher sorption properties. The significant increase is because some chloride can be bounded to the surface of the pore walls. The bounded chloride is then capable of absorbing some water. This phenomenon, therefore, can significantly increase the adsorption properties of the material. The larger sorption as a consequence of the presence of chloride in the sample is also observed in other studies in the literature.

The results show that the new technique is capable of predicting the sorption properties of porous materials with and without chloride.

CRediT authorship contribution statement

A. Taher: Conceptualization, Methodology, Validation, Formal analysis, Investigation, Writing – original draft, Visualization. **H.J.H. Brouwers:** Conceptualization, Methodology, Writing – review & editing, Supervision, Project administration, Funding acquisition.

Declaration of Competing Interest

The authors declare that they have no known competing financial interests or personal relationships that could have appeared to influence the work reported in this paper.

Data availability

Data will be made available on request.

Acknowledgements

The authors would like to acknowledge support from the Dutch Technology Foundation STW. The authors also wish to express their gratitude to Dr. T. Arends, and Dr. A.J.J. van der Zanden for their valuable support during this research.

References

[1] H. Janssen, A discussion of “moisture diffusion in cement pastes with hydrophobic agent”, Constr. Build. Mater. 344 (2022), 128241.
[2] A. Akkaya, İ.H. Çağatay, Investigation of the density, porosity, and permeability properties of pervious concrete with different methods, Constr. Build. Mater. 294 (2021), 123539.
[3] M.H. Nguyen, S. Nishio, K. Nakarai, Effect of temperature on nondestructive measurements for air permeability and water sorptivity of cover concrete, Constr. Build. Mater. 334 (2022), 127361.
[4] A.K. Tedjditi, F. Ghomari, R. Belarbi, R. Cherif, F. Boukhelf, R.T. Bouhraoua, Towards understanding cork concrete behaviour: Impact of considering cork absorption during mixing process, Constr. Build. Mater. 317 (2022), 125905.
[5] V. Baroghel-Bouny, Water vapour sorption experiments on hardened cementitious materials: part I: essential tool for analysis of hygral behaviour and its relation to pore structure, Cem. Concr. Res. 37 (2007) 414–437.
[6] S. Poyet, Experimental investigation of the effect of temperature on the first desorption isotherm of concrete, Cem. Concr. Res. 39 (2009) 1052–1059.
[7] N. De Belie, J. Kratky, S.V. Vlierberghe, Influence of pozzolans and slag on the microstructure of partially carbonated cement paste by means of water vapour and nitrogen sorption experiments and BET calculations, Cem. Concr. Res. 40 (2010) 1723–1733.
[8] J.M. de Burgh, S.J. Foster, Influence of temperature on water vapour sorption isotherms and kinetics of hardened cement paste and concrete, Cem. Concr. Res. 92 (2017) 37–55.
[9] H. Moussaoui, Y. Bahammou, A. Idlimam, A. Lamharrar, Abdenouri N, Investigation of hygroscopic equilibrium and modeling sorption isotherms of the argan products: A comparative study of leaves, pulps, and fruits, Food Bioprod. Process. 114 (2019) 12–22.
[10] L. Wadsö, K. Svennberg, A. Dueck, An experimentally simple method for measuring sorption isotherms, Drying Technol. 22 (2004) 2427–2440.
[11] A.J.J. van der Zanden, E.L.J. Goossens, The measurement of water in paint films, Chem. Eng. Process. 43 (2004) 739–743.
[12] D.P. Broom, Hydrogen storage materials, Gas sorption measurement techniques (Chapter 4), Springer-Verlag, London, 2011, pp. 117–139.
[13] P. Porion, A.M. Faugère, P. Levitz, H. van Damme, A. Raoof, J.P. Guilbaud, F. Chevoir, A NMR investigation of adsorption/desorption hysteresis in porous silica gels, J. Magn. Reson. Imaging 16 (1998) 679.
[14] J. Leisen, B.W. Haskell, M. Benham, Sorption Isotherm Measurements by NMR, Solid State Nucl. Magn. Reson. 22 (2002) 409–422.
[15] A.H. Al-Muhtaseb, W.A.M. McMinn, T.R.A. Magee, Moisture Sorption Isotherm Characteristics of Food Products: A Review, Food Bioprod. Process. 80 (2002) 118–128.
[16] D. Li, Q. Liu, P. Weniger, Y. Gensterblum, A. Busch, B. Krooss, High-pressure sorption isotherms and sorption kinetics of CH4 and CO2 on coals, Fuel 89 (2010).
[17] M. Thommes, K. Kaneko, K. Neimark, V. Alexander, J.P. Olivier, F. Rodriguez-Reinoso, J. Rouquerol, S.W. Kenneth, Physisorption of gases, with special reference to the evaluation of surface area and pore size distribution, Pure Appl. Chem. 87 (2015) 1051–1069.
[18] J. Crank G.S. Park Diffusion in polymers J. Crank G.S. Park Methods of Measurement (Chapter 1) 1968 Academic Press London 1 39.
[19] F. Scarpa, L.A. Tagliafico, A new procedure to measure water adsorption isotherms of porous fibrous materials, J. Porous Mater. 15 (2008) 451–456.
[20] Y. Zhu, X. Wan, X. Han, J. Ren, J. Luo, Q. Yu, Solidification of chloride ions in alkali-activated slag, Constr. Build. Mater. 320 (2022).
[21] L. Bai, J. Xie, J. Liu, Y. Xie, Effect of salt on hygroscopic properties of cement mortar, Constr. Build. Mater. 305 (2021).
[22] H. Sun, S. Liu, F. Yu, X. Zhang, C. Wu, F. Xing, Ren J, Behaviour of cement binder exposed to semi-immersion in chloride-rich salt solutions and seawater with different RH levels, Cem. Concr. Compos. 131 (2022).

[23] L.A. Rijniers, Salt crystallization in porous materials: an NMR study, Eindhoven University of Technology, the Netherlands, 2004. PhD Thesis,.
[24] C. Franzen, P.W. Mirwald, Moisture sorption behaviour of salt mixtures in porous stone, Chem. Erde 69 (2009) 91–98.
[25] M. Koniorczyk, M. Wojciechowski, Influence of salt on desorption isotherm and hygral state of cement mortar – Modelling using neural networks, Constr. Build. Mater. 23 (2009) 2988–2996.
[26] C. Villani, R. Spragg, M. Pour-Ghaz, W.J. Weiss, The role of deicing salts on the non-linear moisture diffusion coefficient of cementitious materials, Brittle Matrix, Composites 10 (2012) 101–114.
[27] NT Build 492, Concrete, mortar and cement-based repair materials: Chloride migration coefficient from non-steady-state migration experiments. Nord test method. Finland, (1999).
[28] ASTM C1202 Standard Test Method for Electrical Indication of Concrete's Ability to Resist Chloride Ion Penetration Annual Book of ASTM Standards. American Society for Testing and Materials 04.02 2005 Philadelphia, USA.
[29] Q.L. Yu Design of environmentally friendly calcium sulfate-based building materials - Towards an improved indoor air quality 2012 Eindhoven University of Technology the Netherlands PhD thesis.
[30] A. Townshend, Titrimetric analysis, Encyclopedia of analytical science, Academic Press 9 (1995) 5240–5248.
[31] P. Parvinen, V. Virtanen, L.H.J. Lajunen, Chlorine, in: A. Townshend (Ed.), Encyclopedia of Analytical Science, Academic Press, 1995, pp. 687–699.
[32] A. Hulanicki, S. Glab, Potentiometry: Titrations, in: A. Townshend (Ed.), Encyclopedia of Analytical Science, Academic Press, 1995, pp. 4106–4112.
[33] J.A. Dean, Electroanalytical methods, Analytical Chemistry Handbook (1995) 14.48.
[34] R.C. Reid, J.M. Prausnitz, T.K. Sherwood, The pressure of gases and liquids, 3rd edition, McgrawHill Book Cy, New York, 1977.
[35] O.C. Bridgeman, E.W. Aldrich, Vapor Pressure Tables for Water, J. Heat Transfer 86 (1964) 279–286.
[36] S.J. Gregg, K.S.W. Sing, Adsorption, Surface Area and Porosity, 2nd edition, Academic Press, London, 1982.
[37] S. Brunauer, P.H. Emmett, E. Teller, Adsorption of gases in multimolecular layers, J. Am. Chem. Soc. 60 (1938) 309–319.
[38] D. Benavente, M.A. Garcia del Cura, A. Bernabeu, S. Ordonez, Quantification of salt weathering in porous stones using an experimental continuous partial immersion method, Eng. Geol. 59 (2001) 313–325.
[39] D. Benavente, M.A. Garcia del Cura, S. Ordonez, Salt Influence on evaporation from porous building rocks, Constr. Build. Mater. 17 (2003) 113–122.
[40] A. Selander, Hydrophobic impregnation of concrete structures, Effect on concrete properties, Royal Institute of Technology, Stockholm, Sweden, 2010. Ph.D. Thesis.
[41] R. Spragg, J. Castro, W. Li, M. Pour-Ghaz, P.T. Huang, J. Weiss, Wetting and drying of concrete using aqueous solutions containing deicing salts, Cem. Concr. Compos. 33 (2011) 535–542.
[42] S. Tada, Watanabe K, Dynamic determination of sorption isotherm of cement-based materials, Cem. Concr. Res. 35 (2005) 2271–2277.
[43] J.F. Daian, Condensation and isothermal water transfer in cement mortar, Transp. Porous Media 3 (1988) 563–589.
[44] L. Pel, Moisture transport in porous building materials, Eindhoven University of Technology, the Netherlands, 1995. PhD Thesis.
[45] H.J.H. Brouwers, The work of Powers and Brownyard revisited: Part 1, Cem. Concr. Res. 34 (2004) 1697–1716.
[46] H.J.H. Brouwers. A hydration model for Portland cement using the work of Powers and Brownyard, Eindhoven University of Technology/Portland Cement Association Report SN3039, 2011.